NATURAL SCIENCE REVIEW 3 200902 (2026)
nsr.jinr.int

Recent advances in the gauge field decomposition into confining and nonconfining components in nonabelian gauge theories

V. Bornyakov*[1] and I. Kudrov[1]

[1] *National Research Center "Kurchatov Institute" — A. A. Logunov Institute for High Energy Physics, Protvino, 142281 Russia*

Abstract

We present a short review of recent studies of the gauge field decomposition into confining and nonconfining components in nonabelian gauge theories after fixing the maximal Abelian gauge. This subject is closely related to the dual superconductor scenario of confinement, one of the fundamental nonperturbative properties of QCD, and we give a short review of this scenario. The lattice regularization of QCD, or simply lattice QCD (LQCD), is used in these studies. It is well known that LQCD provides a first-principles approach to the computation of many physical observables in QCD, such as the hadron spectrum, quark masses, the running coupling constant, etc. Lattice QCD also provides a method to study important fluctuations of the gauge field and thus to try to understand which fluctuations are playing the most important role for one phenomenon or another in QCD.

Keywords: quantum chromodynamics, confinement, monopoles, maximal Abelian gauge

DOI: 10.54546/NaturalSciRev.200902

1. Introduction

The success of the Standard Model is, to a large extent, due to perturbation theory. In particular, it is experimentally well established that strong interactions are described to a very high precision by quantum chromodynamics (QCD), a nonabelian gauge theory of quarks and gluons with gauge group $SU(3)$. But QCD has many nonperturbative properties since the running coupling $\alpha_s(r)$ is large at large distances/small momenta. The two fundamental properties of QCD, confinement of color and spontaneous chiral symmetry breaking, are to be studied using a nonperturbative method. The lattice regularization, or simply lattice QCD (LQCD), is one of the nonperturbative approaches formulated from the first principles of quantum field theory.

LQCD has been successfully used for studies of both the confinement mechanism and chiral symmetry breaking. In relation to these problems, the following types of nontrivial fluctuations of the gauge field were studied on a lattice: instantons [1], calorons [2], dyons [3], color-magnetic monopoles [4, 5], center vortices [6, 7], and their interrelations [8, 9]. These studies were

*Corresponding author e-mail address: vitaly.bornyakov@ihep.ru

Received: 1 October 2026; Revised: 28 October 2026; Accepted: 12 November 2026; Published: 27 November 2026
Copyright: © by the author(s), 2026, under license to Joint Institute for Nuclear Research. This article is an open access article distributed under the terms and conditions of the Creative Commons Attribution-NonCommercial 4.0 International license (CC BY-NC License 4.0).

comprehensively reviewed in the following review papers: [10–12] (dual superconductor scenario of confinement), [13, 14] (mostly on center vortex picture of confinement), [15] (monopole confinement and relation between confinement and chiral symmetry breaking).

In this paper, we review recent results on the gauge field decomposition in the maximal Abelian gauge (MA gauge, MAG) obtained in the context of the dual superconductor scenario of confinement. The paper is organized as follows. We start by introducing the LQCD in the next section, including the gauge fixing procedure on a lattice. Then, in Section 3, we explain the main ideas of the dual superconductor scenario of confinement and the main results obtained in the study of these ideas. Section 4 is devoted to the gauge field decomposition in $SU(2)$ gluodynamics and in $SU(2)$ QCD. In Section 5, results for the gauge field decomposition in $SU(3)$ gluodynamics and the problem of Gribov copies are presented. We briefly draw the conclusions in the final section.

2. Lattice regularization of QCD

To study QCD in a mathematically rigorous way, lattice QCD formulated by K.Wilson [16] is unique. The most important features of LQCD are the transition to Euclidean space, the replacement of the four-dimensional spacetime continuum by a hypercubic lattice, and the definition of quark and gauge fields on the sites and links of this lattice, respectively. Finite lattice spacing ensures the regularization of ultraviolet divergences, and the functional integral becomes a finite-dimensional integral. Thus, LQCD is mathematically rigorously defined.

It is important that this finite-dimensional integral can be computed numerically using Monte Carlo method. At zero quark chemical potential, all systematic and statistical errors are under control and can be reduced by using more computing power or more effective algorithms.

LQCD is now accepted as a first principles tool to compute QCD predictions for many hadron properties, such as the hadron spectrum, decay constants, form factors, strong coupling, transition temperature, and others. At the same time, LQCD allows one to answer important qualitative questions about the fluctuations that provide QCD with its properties.

The lattice gauge field $U_\mu(x) \in SU(3)$ is defined on the links connecting the sites x and $x + a\hat{\mu}$, where a is the lattice spacing (see Figure 1). $U_\mu(x)$ is related to the vector potential $A_\mu(x)$ by the relation

$$U_\mu(x) = P\exp\left(i \int_{C_{x,x+a\hat{\mu}}} gA_\mu(s)ds \right) \approx 1 + iagA_\mu(x) + O(a^2)\,. \tag{1}$$

The Wilson action for a lattice gauge field is

$$S_W = \beta \sum_{x,\mu<\nu} (1 - \frac{1}{N_c}\mathrm{ReTr}U_{\mu\nu}) = a^4 \left(\frac{\beta}{2N_c} \sum_{x,\mu<\nu} \mathrm{Tr}[F_{\mu\nu}^2] + O(a^2) \right), \quad \beta = 2N_c/g^2\,, \tag{2}$$

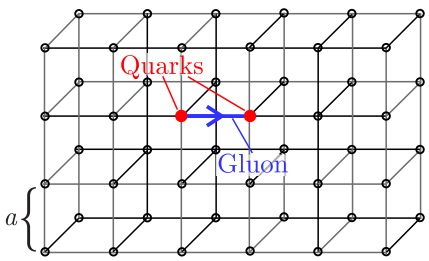


Figure 1. 3D slice of 4D lattice.

where $U_{\mu\nu}(x) = U_\mu(x)U_\nu(x+a\hat{\mu})U^\dagger_\mu(x+a\hat{\nu})U^\dagger_\nu(x)$. The lattice fermion action has the general form

$$S_F = \sum_{x,y} \bar{\psi}_x M_{xy}(U)\psi_y \,, \tag{3}$$

where $\bar{\psi}_x, \psi_y$ are anticommuting Grassmann variables defined at each lattice site, belonging to the fundamental representation of the gauge group; $M_{xy}(U)$ is a discretization of the Dirac operator, a matrix with coordinate, spin, color, and flavor indices. The original Wilson lattice fermion action is

$$S_{FW} = a^4 \sum_x \left[\bar{\psi}_x \left(m + \frac{4r}{a} \right) \psi_x + \frac{1}{2a} \sum_\mu \left(\bar{\psi}_x (\gamma_\mu - r) U_\mu(x) \psi_{x+a\hat{\mu}} - \bar{\psi}_{x+a\hat{\mu}} (\gamma_\mu + r) U^\dagger_\mu(x) \psi_x \right) \right]. \tag{4}$$

Both (2) and (4) are gauge invariant. It should be noted that for both the lattice gauge action S_G and the lattice fermion action S_F there exist alternative formulations that are superior to the versions of the actions (2) and (4) originally proposed by K. Wilson. In section 4 we will discuss results obtained with tadpole improved gauge field action and also improved fermionic action with another type of discretization introduced by Kogut and Susskind [17].

The physical observable is calculated as follows:

$$\langle \mathcal{O}(U, \bar{\psi}, \psi) \rangle = \frac{1}{Z} \int \mathcal{D}U \; e^{-S_G(U)} \mathrm{det} M(U) \; \mathcal{O}(U, M^{-1}(U)).$$

In this expression, the integral over fermion fields was evaluated analytically. On a finite-size lattice, this is a finite-dimensional integral of large dimension ($\sim O(10^9)$). To calculate this integral, a Monte Carlo method is used, an essential element of which is importance sampling. A Markov chain of lattice gauge field configurations is generated with probability

$$P\{U\} \propto e^{-S_{\text{eff}}(U)} \,, \tag{5}$$

where $S_{\text{eff}}(U) = S_G(U) - \log(\det M(U))$. To evolve the gauge field without significantly changing $S_{\text{eff}}(U)$, the molecular dynamics method is used, each trajectory ending with an accept–reject Metropolis step. For an observable containing fermionic fields, it is necessary to calculate the inverse Dirac matrix, M^{-1}, which, along with generating gauge field configurations, is a task that requires significant computer resources. The average $\langle \mathcal{O} \rangle$ is then computed as a sum over generated configurations of the gauge field:

$$\langle \mathcal{O} \rangle \approx \frac{1}{N_{\text{conf}}} \sum_{i=1}^{N_{\text{conf}}} \mathcal{O}_i(U) \,, \tag{6}$$

where $\mathcal{O}_i(U)$ is the value of observable $\mathcal{O}(U)$ on configuration number i and N_{conf} is the number of statistically independent configurations.

Note that the value $\beta = 6/g^2$ implicitly fixes the lattice spacing a and the QCD coupling constant $\alpha_s(a)$. To determine the lattice spacing a in physical units, an experimental value, for example, of the mass m_Ω is used: $m_\Omega^{latt} = a m_\Omega$. In the case of gluodynamics, the Sommer parameter $r_0 = 0.5$ fm is determined from the interaction potential $V(r)$ between a static quark and antiquark by this relation

$$r_0^2 F(r_0) = 1.65, \qquad F(r) = \frac{dV(r)}{dr} \tag{7}$$

is used. The static potential $V(r)$ used in this definition is computed from the Wilson loop as $V(r) = -\lim_{t\to\infty} \frac{1}{t} \log W(r,t)$, $\quad W(C) = \frac{1}{N_c} \mathrm{Tr} \prod_{l\in C} U_l$.

To finalize the computation of the given observable, the two limits should be undertaken: the continuum limit $a(\beta) \to 0$ and the infinite volume limit $L_s \to \infty$, where L_s is the lattice size in spatial directions in physical units.

It is well known that LQCD provides a first-principles approach to the computation of many physical observables in QCD, such as the hadron spectrum, quark masses, decay constants, the running coupling, semileptonic form factors, etc. [18]. For the studies of QCD vacuum properties and, in particular, for the purpose of clarifying the color-confinement mechanism rigorously, Monte Carlo numerical simulations in the framework of lattice QCD seem to be a unique method.

LQCD is formulated in a gauge invariant way, and to compute the gauge invariant observables, gauge fixing is not needed. However, gauge fixing is needed to compute gauge dependent quantities, e.g., field propagators and vertices. These quantities are of fundamental interest. In particular, the respective lattice results are used in other nonperturbative approaches, such as Dyson–Schwinger equations, the functional renormalization group, and effective field theories.

For quite a long time, the numerical procedure of gauge fixing in lattice regularization was based on the expression introduced in [19] (here we omit the quark fields for simplicity)

$$\langle \mathcal{O} \rangle = \frac{1}{Z} \int DA e^{-S(A)} \mathcal{O}(A^{g(A)}) \,, \tag{8}$$

where $\mathcal{O}(\mathcal{A})$ is some gauge noninvariant observable and $g(A)$ is the gauge transformation satisfying the gauge condition $f(A^{g(A)}) = 0$. For the gauge without Gribov copies, this is the correct expression, while for the gauge with Gribov copies, the problem of their effect persists.

One definition for the nonperturbative gauge fixing was introduced in [20, 21]:

$$\langle \mathcal{O} \rangle = \frac{1}{Z(\lambda)} \int DA \; e^{-S(A)} \; I^{-1}(A) \int Dg \; e^{-\lambda F(A^g)} \mathcal{O}(A^g) \,, \tag{9}$$

where λ is gauge parameter and $\mathcal{O}$ is some observable,

$$I(A) = \int Dg \; e^{-\lambda F(A^g)} \,. \tag{10}$$

Here $F(A)$ is a functional whose extrema satisfy gauge condition $f(A^{g(A)}) = 0$. The limit $\lambda \to \infty$ corresponds to integration over the fundamental modular domain. Constraining to this domain as a way to solve the Gribov copies problem was suggested in [22] and later this idea was extended in [23] to the lattice simulations in the case of Landau and Coulomb gauges.

It is impossible to find the global minima of $F(A)$ numerically. One can assume that generating many such minima and taking the lowest of them one approaches the global one. Such a practical recipe was formulated in [24] where MAG was studied in $SU(2)$ gluodynamics. It was demonstrated in [24] that in MAG the effects of Gribov copies, i.e., dependence of gauge noninvariant observables on the choice of Gribov copies, are strong. This recipe was then used in further studies of MAG both in gluodynamics and in QCD [25–28]. It was also adopted for other gauges [29], in particular, Landau gauge [30, 31], Coulomb gauge [32], and center gauges [33, 34]. In Section 4, where results for $SU(2)$ gauge group are presented, we follow this approach. In the case of $SU(3)$ gluodynamics, discussed in Section 5, we show that another approach to the Gribov copy choice is needed to obtain proper decomposition of the gauge field.

3. Dual superconductor scenario of confinement

Mandelstam [35] and 't Hooft [36] proposed a dual picture of the Meissner effect as the quark confinement mechanism, assuming that the condensation of the color-magnetic monopoles forces the color-electric field to form color flux tubes, similarly to magnetic flux tubes in the Abelian Higgs model with a charged Higgs field.

It is known that the monopole solution with finite energy exists in $SU(2)$ Higgs model with adjoint Higgs field [37, 38]. There is no Higgs field in QCD to define color-magnetic monopoles. 't Hooft [39] suggested introducing the Abelian subgroup necessary to define monopoles by fixing the gauge that leaves unbroken the maximal Abelian subgroup $U(1)^{N_c-1}$. Any operator in the adjoint representation can be used to define such a gauge by diagonalization of this operator. Examples of such operators are $F_{\mu\nu}(x)$ or the Polyakov loop $P(x)$. It has been shown that fixing such a gauge leads to the appearance of singularities at points where two or more eigenvalues coincide. In the vicinity of the singularity, the gauge field takes the form of a 't Hooft–Polyakov monopole. Note, however, that far from this point, the form of the gauge field is not fixed in the general case; that is, properties characteristic of a magnetic monopole manifest only in the neighborhood of the singularity. In general, no connection has been established between the Abelian monopoles defined in this way and solutions to the classical equations of motion. Although such a connection exists in certain specific cases, it is more appropriate to view these monopoles as a type of quantum fluctuations. 't Hooft hypothesized that monopoles defined in this manner play an important role, particularly regarding the problem of confinement.

't Hooft also suggested the covariant gauge which breaks $SU(N_c)$ to $U(1)^{N_c-1}$. This is the MA gauge. In the case of $N_c = 2$, the gauge condition in the differential form is

$$(\partial_\mu \pm igA^3_\mu(x))A^\pm_\mu(x) = 0, \qquad A^\pm_\mu(x) = A^1_\mu(x) \pm iA^2_\mu(x)\,. \tag{11}$$

These equations are satisfied by the extrema of the functional

$$F(A) = \frac{1}{8V}\int d^4x \sum_{\mu=1}^{4}(A^1_\mu(x)^2 + A^2_\mu(x)^2). \tag{12}$$

On the lattice, the monopoles are identified via their Dirac string. This definition was introduced for lattice monopoles in a theory with the U(1) gauge group in [40] and is also used for the nonabelian groups after Abelian projection. The dynamical variables in such a model are angles $\theta_\mu(x) \in [-\pi, \pi)$ defined on the lattice links. The Abelian plaquette variables,

$$\theta_{\mu\nu}(x) = \partial_\mu\theta_\nu(x) - \partial_\nu\theta_\mu(x) \equiv \theta_\nu(x+\hat{\mu}) - \theta_\nu(x) + \theta_\mu(x) - \theta_\mu(x+\hat{\nu}), \tag{13}$$

$\theta_{\mu\nu}(x) \in [-4\pi, 4\pi)$, are decomposed into a periodic (regular) component $\bar{\theta}_{\mu\nu}(x) \in [-\pi, \pi)$ and a singular component $m_{\mu\nu}(x) = 0, \pm1, \pm2$:

$$\theta_{\mu\nu}(x) = \bar{\theta}_{\mu\nu}(x) + 2\pi m_{\mu\nu}(x). \tag{14}$$

This equation is the lattice version of the continuum equation for the field strength tensor in the presence of a Dirac string. $\bar{\theta}_{\mu\nu}(x)$ describes the $U(1)$-invariant electromagnetic flux through the plaquette, and $2\pi m_{\mu\nu}$ represents the magnetic flux from Dirac strings, such that $|m_{\mu\nu}(x)|$ equals the number of Dirac strings passing through the plaquette. Magnetic monopole currents $k_\mu(x^*)$ are defined on the links of the dual lattice, i.e., the lattice obtained by translating the original lattice by the vector $\delta = \{1/2, 1/2, 1/2, 1/2\}$. The currents $k_\mu(x^*)$ are defined as follows:

$$k_\mu(x^*) = \frac{1}{4\pi}\varepsilon_{\mu\nu\rho\sigma}\partial_\nu\bar{\theta}_{\rho\sigma}(x), \tag{15}$$

In the following, we will use the same notation for the sites of the original and dual lattices. It is evident that the current $k_\mu(x)$ is conserved:

$$\partial_\mu k_\mu(x) = 0. \tag{16}$$

Let us note that shifted currents

$$k'_\mu(x) = k_\mu(x + \hat{\mu}) \tag{17}$$

satisfy different conservation condition: $\partial^-_\mu k'_\mu(x) = 0$, where ∂^-_μ is lattice backward derivative, and thus form closed loops which combine into clusters. In the continuum limit $k_\mu(x)$ and $k'_\mu(x)$ coincide. It is well known that the color-magnetic currents form one large, percolating, cluster and many small clusters. The percolating cluster is responsible for the monopole string tension $\sigma_{\rm mon}$; for this reason, the respective currents are called infrared monopoles.

The MA gauge defined in Eq. (11) was found to be a suitable gauge to study the dual superconductor scenario of confinement. First, the Abelian dominance predicted in [41] was discovered [42] in this gauge. It was demonstrated both in gluodynamics [24, 26, 42–45] and in QCD [28] that the Abelian string tension σ_{ab} calculated from the Abelian Wilson loops approximate the nonabelian string tension σ well. It was further discovered [24, 46, 47] that the monopole static potential $V_{\rm mon}(r)$ (the definition will be given later) also has a string tension $\sigma_{\rm mon}$ close to the nonabelian one. It is believed that these and similar observations give support to conjecture that monopole degrees of freedom are indeed responsible for confinement, see [10–12, 15, 48, 49] for reviews.

In the case of $SU(2)$ gluodynamics, it was demonstrated [44] using the gauge fixing procedure described above that, while $\sigma_{ab} \sim 0.9\sigma$ at finite lattice spacing, $\sigma_{ab} = \sigma$ within error bars in the continuum limit. In contrast, in $SU(3)$ gluodynamics, this issue has not been resolved until recently. Results for the ratio σ_{ab}/σ in SU(3) gluodynamics were presented in [26, 28, 45]. As was found in [26, 28] σ_{ab}/σ was substantially lower than 1.0 at least at lattice spacing $a \approx 0.09$ fm ($\beta = 6.0$). Later, this ratio was computed in [45], where few lattice spacings and various physical volumes were considered. The conclusion was made that perfect agreement of σ_{ab} with physical string tension σ (and thus perfect Abelian dominance) can be observed in $SU(3)$ gluodynamics on sufficiently large lattices. Below, in section 5, we will present results [50, 51] demonstrating that indeed one can achieve this perfect agreement in $SU(3)$ gluodynamics. However, to accomplish this, it is necessary to choose proper Gribov copies rather than to eliminate finite volume effects. The same conclusion was made [51] for the monopole string tension $\sigma_{\rm mon}$.

The Abelian and monopole dominance were also demonstrated for other observables: chiral condensate, topological charge, and deconfinement transition temperature [52–57]. The important result obtained numerically in both $SU(2)$ [27, 58, 59] and $SU(3)$ [60] gluodynamics was that the infrared effective action for gluodynamics is indeed the dual Abelian Higgs model.

In Sections 4 and 5, we will work with the MA gauge. This is supported by the lattice numerical results [61], which show that fixing the MA gauge and doing subsequent Abelian projection is a tool to locate the color-magnetic monopoles as Dirac monopoles using the technique developed in [40] for compact $U(1)$ theory. The gauge invariance of the dual superconductor properties of the QCD vacuum is also supported by numerical results on the monopole condensation presented in a series of papers by A. Di Giacomo and collaborators in [62–65]. The operator $\hat{\mu}$ that creates a monopole was defined as the shift of the vector potential by the classical field of the monopole (similarly to definition formulated in [66] for $U(1)$ theory). It was then shown numerically that $\langle\hat{\mu}\rangle$ is nonzero in the confinement phase and zero in the deconfinement one, independent of gauge fixing.

New approach to the problem was formulated by T. Suzuki and collaborators [67]. The idea of gauge-independent Abelian magnetic monopoles in QCD was proposed. The essential assumption is that gauge fields contain a singularity of the Dirac type. Then non-Abelian Bianchi identity is violated and the violation (VNABI) $J_\mu(x)$ is found to be equivalent to N_c^2-1 conserved Abelian magnetic monopole currents $k_\mu^a(x)$. It was shown in $SU(2)$ and in $SU(3)$ gluodynamics, that independent of any gauge fixing the longitudinal electric field and the surrounding monopole currents have properties consistent with the dual Meissner picture [68, 69].

4. Decomposition for $SU(2)$ gluodynamics and $SU(2)$ QCD

4.1. Definitions and simulation details

In this section, we consider the gauge field decomposition in $SU(2)$ gluodynamics and in $SU(2)$ QCD. The MA gauge is fixed numerically by finding minima with respect to gauge transformations $U_\mu(x) \to g^\dagger(x)U_\mu(x)g(x+\mu)$ of the functional

$$F_{\text{lat}}(U) = 1 - \frac{1}{8N_{\text{sites}}} \sum_{x,\mu} \text{Tr}\left(\sigma_3 U_\mu(x)\sigma_3 U_\mu(x)^\dagger\right), \tag{18}$$

which converges in the $a \to 0$ limit to the respective continuum functional:

$$\frac{1}{a^2}F_{\text{lat}}(U) = \frac{1}{8V}\int_V d^4x \sum_{\mu=1}^{4}(A_\mu^1(x)^2 + A_\mu^2(x)^2) + O(a^2). \tag{19}$$

There were two methods utilized to find the minima of the functional (18). The first one is the relaxation method. This method involves the local maximization of the functional relative to the gauge transformation $g(x)$ on a site x

$$F_x^{\text{loc}}(U) = \sum_\mu \text{Tr}\left(\sigma_3 g(x)U_\mu(x)\sigma_3 U_\mu^\dagger(x)g^\dagger(x) + \sigma_3 U_\mu^\dagger(x-\hat{\mu})g(x)\sigma_3 g^\dagger(x)U_\mu(x-\hat{\mu})\right). \tag{20}$$

This local maximization step is applied iteratively until the average deviation $1 - \frac{1}{8N_{\text{sites}}} \times$ $\times \sum_x \text{Tr}(g(x)) < \epsilon$ is reached, with a typical value $\epsilon = 10^{-14}$. To enhance the effectiveness of the search for the gauge configuration yielding the global minimum of the functional, an over-relaxation method is additionally used. In alternation with the local maximization step, the nontrivial gauge transformation is found that gives the same value of the local functional (20). It helps to search through the configuration space more effectively. The combination of these methods is called the relaxation–over-relaxation (RO) algorithm.

To find the minima more effectively, another algorithm was used in addition to the RO method. This is the simulated annealing (SA) algorithm. This algorithm requires the introduction of a dimensionless parameter called temperature T_{SA}. The algorithm generates the gauge transformation with a probability distribution

$$P(U) \propto \exp(-F(U)/T^{\text{SA}}). \tag{21}$$

The SA algorithm is usually implemented by iteratively applying a heat bath step, which locally generates a new gauge transformation $g(x)$ so that the new functional is locally distributed as $P \propto \exp(F_x^{\text{loc}}(U)/T^{\text{SA}})$. At the beginning, the temperature T^{SA} is set to a sufficiently large value. In the case of $SU(2)$ gluodynamics, it was chosen to be $T^{\text{SA}} = 2.5$. The temperature is gradually decreased to a sufficiently low value, which is also chosen empirically. At a low

enough value of $T_{\rm SA}$, the SA algorithm is similar to relaxation, i.e., local maximization of expression (20). To optimize the search through the configuration space of the gauge transformation, over-relaxation is used as in the case of relaxation. After the SA algorithm is finished, the RO algorithm is applied in order to complete the minimization of the functional (18). Similarly, this procedure can be repeated starting from a random gauge configuration, and the gauge configuration with the lowest value of the functional can be chosen.

In [70], the SA method, followed by the RO method, was used. The SA temperature was varied in a range $T^{\rm SA} = 2.5 - 0.1$, and for every four steps of relaxation, one step of over-relaxation was applied for both SA and RO. In a range of $T^{\rm SA} \approx 1.4$, the functional (18) experiences rapid change due to the fact that the gauge transformation $g(x)$, with the functional (18) acting as a spin action, is equivalent to a spin system that exhibits a phase transition in that range of temperatures.

After the gauge is fixed, the coset decomposition is made:

$$U_\mu(x) = C_\mu(x) u_\mu(x)\,, \tag{22}$$

where $u_\mu(x) \in U(1)$ and $C_\mu(x) \in SU(2)/U(1)$. Eq. (22) defines the Abelian projection for the lattice gauge field. Values of the functional are shown in Table 1.

Table 1. Values of the functional (18) for $SU(2)$ gluodynamics.

β	$F_{\rm lat}(U)$
2.4	0.266148(39)
2.5	0.248671(39)
2.6	0.233582(36)

The Abelian gauge field can be further decomposed into the monopole (singular) component $u^{\rm mon}_\mu(x)$ and the photon (regular) component $u^{ph}_\mu(x)$ [71]:

$$u_\mu(x) = u^{\rm mon}_\mu(x) u^{ph}_\mu(x)\,. \tag{23}$$

In terms of the corresponding angles defined as $u_\mu(x) = {\rm diag}(e^{i\theta_\mu(x)}, e^{-i\theta_\mu(x)})$ and similarly for $u^{{\rm mon},ph}_\mu(x)$, this decomposition reads

$$\theta_\mu(x) = \theta^{\rm mon}_\mu(x) + \theta^{ph}_\mu(x)\,, \tag{24}$$

It was shown in [71] that $\theta^{\rm mon}_\mu(x)$ can be expressed in terms of the Dirac plaquette variables $m_{\nu\mu}(x)$:

$$\theta^{\rm mon}_\mu(x) = -2\pi \sum_y D(x-y)\partial'_\nu m_{\nu\mu}(y)\,, \tag{25}$$

where $D(x)$ is the lattice inverse Laplacian, ∂'_ν is the lattice backward derivative, and $m_{\mu\nu}(x)$ and $\theta_{\mu\nu}(x)$ are defined in the same way as in $U(1)$ theory by DeGrand–Toussaint (13), (14). This solution satisfies the Lorenz gauge condition $\partial'_\mu \theta_{\rm mon}(s,\mu) = 0$.

The decomposition of the $SU(2)$ gauge field into confining and nonconfining components is then defined by

$$U_\mu(x) = \tilde{U}_\mu(x) u^{\rm mon}_\mu(x)\,, \tag{26}$$

where $u^{\rm mon}_\mu(x)$ is a confining field that produces almost all of the monopoles and $\tilde{U}_\mu(x) \in SU(2)$ is the modified gauge field that produces (almost) no monopoles and is nonconfining, as we show later.

As mentioned above, the MA gauge is fixed up to residual $U(1)$ symmetry. The Abelian angle transforms under $U(1)$ as

$$\theta'_\mu(x) = \theta_\mu(x) + \partial_\mu w(x) + 2\pi n_\mu(x)\,, \tag{27}$$

where $\theta'_\mu(x)$, $w(x) \in (-\pi, \pi]$, $n_\mu(x)$=0, ± 1.

It was shown in [72] that $W_{\rm mod}(r,t)$ is not invariant under gauge transformations (27) with $n_\mu(x) = \pm 1$. To eliminate such transformations, one can use the Landau gauge fixing, which is defined by a functional

$$F^{\rm Landau}(\theta) = \sum_{x,\mu} \cos(\theta_\mu(x))\,. \tag{28}$$

Maximization of the functional (28) relative to $w(x)$ fixes the gauge completely.

We define the decomposition of the static potential as an approximate relation that corresponds to the decomposition (26)

$$V(r) \approx V_{\rm mon}(r) + V_{\rm mod}(r)\,, \tag{29}$$

where $V(r), V_{\rm mon}(r), V_{\rm mod}(r)$ are static potentials between quarks obtained from the original non-abelian gauge field, monopole field, and modified field, respectively. The static potentials are extracted from Wilson loops calculated using the corresponding fields.

4.2. Results

The decomposition was tested with the Wilson lattice action at $\beta = 2.4, 2.5$ on 24^4 lattice and at $\beta = 2.6$ on the 32^4 lattice using 100 statistically independent configurations. With the tadpole improved action, the simulations were conducted at $\beta = 3.4$ on 24^4 lattices. The simulations in the QC_2D were made on the 32^4 lattice with small lattice spacing [73]. To fix MAG, the simulated annealing algorithm [24, 74] with one gauge copy was used.

The generated configurations were decomposed into monopole and modified configurations, and $r \times t$ rectangular Wilson loops $W(r,t)$, $W_{\rm mon}(r,t)$, and $W_{\rm mod}(r,t)$ were calculated. Obtained potentials $V(r)$, $V_{\rm mon}(r)$, and $V_{\rm mod}(r)$ are shown in Figure 2, Figure 3, and Figure 4.

An example of the decomposition for simulations with Wilson action at $\beta = 2.6$ is shown in Figure 2 (left), where it can be seen that the approximate relation (29) is satisfied with good accuracy. Comparison of the nonabelian potential $V(r)$ with the sum $V_{\rm mod}(r) + V_{\rm mon}(r)$ for three values of β is shown in Figure 2 (right). All the potentials were fitted to the Cornell potential

$$V(r) = V_0 + \alpha/r + \sigma r\,, \tag{30}$$

where α is the Coulomb coefficient, σ is the string tension, and V_0 is the self energy. The parameters of the fit are shown in Table 2. The solid curve in Figure 2 shows the fit to Eq. (30) at $\beta = 2.6$ for both plots, and the two dashed curves show its Coulomb and linear terms with adjusted constants. The data points are shifted by a constant that is defined by the value of the nonabelian potential $V(r)$ at $r = 1/\sqrt{\sigma}$ at the corresponding value of β.

One of the properties of the decomposition found for $SU(2)$ gluodynamics is that the decomposition becomes more accurate with $\beta \to \infty$. To show this thoroughly, the relative deviation of the decomposition was calculated as

$$\Delta(r) = \frac{V(r) - (V_{\rm mon}(r) + V_{\rm mod}(r))}{V(r)} \tag{31}$$

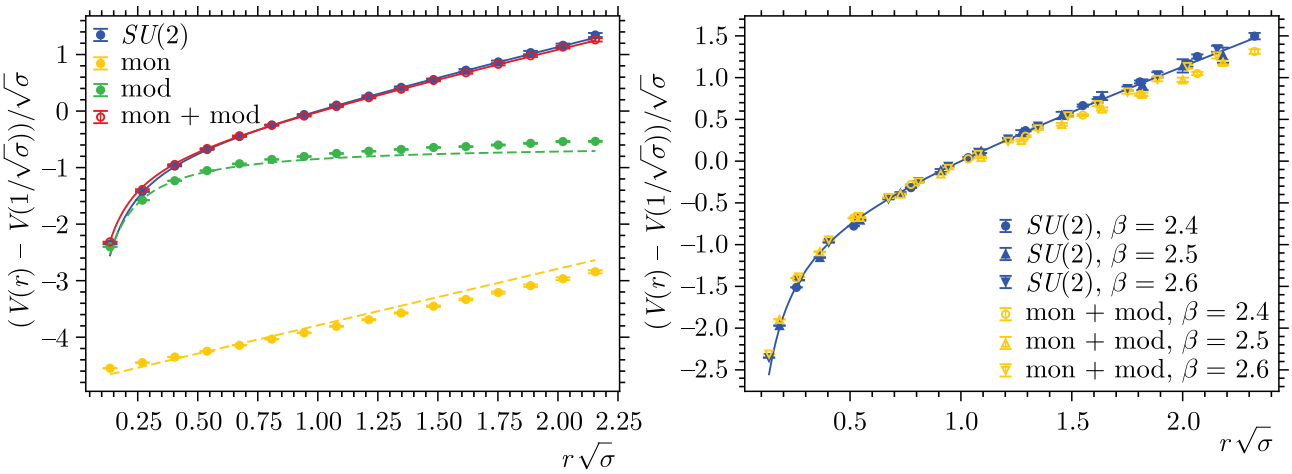


Figure 2. Comparison of the nonabelian potential $V(r)$ (blue) with the monopole potential $V_{\rm mon}(r)$ (yellow), the modified potential $V_{\rm mod}(r)$ (green), and the sum $V_{\rm mod}(r)+V_{\rm mon}(r)$ (red) for $\beta = 2.6$ (left), and comparison of the nonabelian potential $V(r)$ (filled blue symbols) with the sum $V_{\rm mod}(r)+V_{\rm mon}(r)$ (empty yellow symbols) for $\beta = 2.4, 2.5, 2.6$ (right). The solid curve shows the fit to Eq. (30) at $\beta = 2.6$ for both plots. Two dashed curves show its Coulomb and linear terms with adjusted constants. The data points are shifted by a constant that is defined by the value of the nonabelian potential $V(r)$ at $r = 1/\sqrt{\sigma}$ at the corresponding value of β.

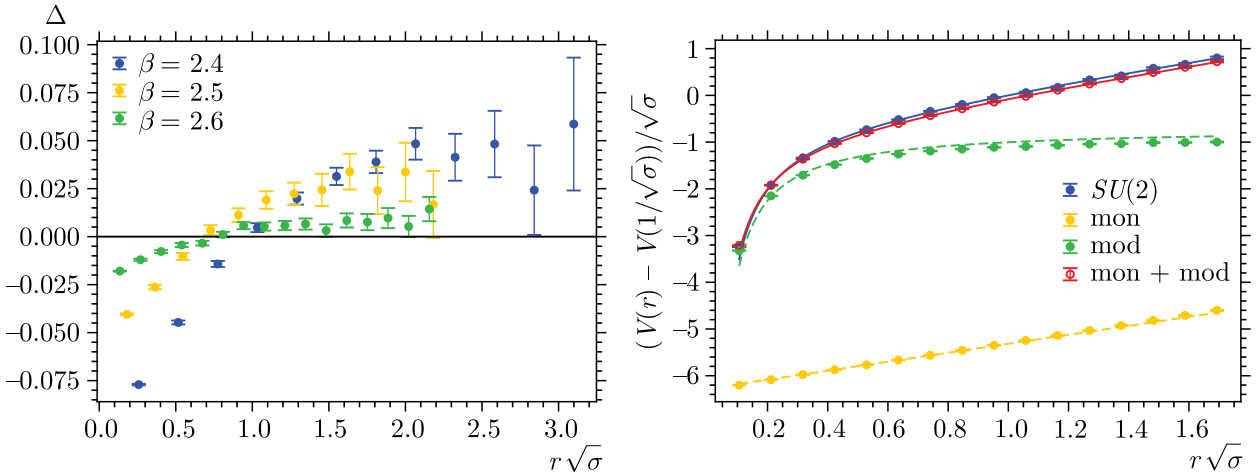


Figure 3. The relative deviation (31) for $\beta = 2.4, 2.5, 2.6$ (left). Comparison of the nonabelian potential $V(r)$ (blue) with the monopole potential $V_{\rm mon}(r)$ (yellow), the modified potential $V_{\rm mod}(r)$ (green), and the sum $V_{\rm mod}(r) + V_{\rm mon}(r)$ (red) for $SU(2)$ QCD with dynamical quarks (right). The solid curve and dashed curves carry the same meaning as in Figure 2. The data points in the right plot are shifted as in Figure 2.

Table 2. Parameters of the potentials obtained by fits to the function (30).

Potential	$\beta = 2.4$		$\beta = 2.5$		$\beta = 2.6$	
	σa^2	α	σa^2	α	σa^2	α
V	0.067(1)	–0.31(1)	0.033(1)	–0.290(4)	0.0184(5)	–0.25(1)
$V_{\rm mon} + V_{\rm mod}$	0.058(1)	–0.27(1)	0.030(1)	–0.27(1)	0.0175(4)	–0.25(1)
$V_{\rm mon}$	0.060(1)	–0.002(1)	0.030(1)	0.015(3)	0.0167(6)	0.06(2)
$V_{\rm mod}$	—	–0.25(1)	—	–0.27(1)	0.002(1)	–0.27(1)

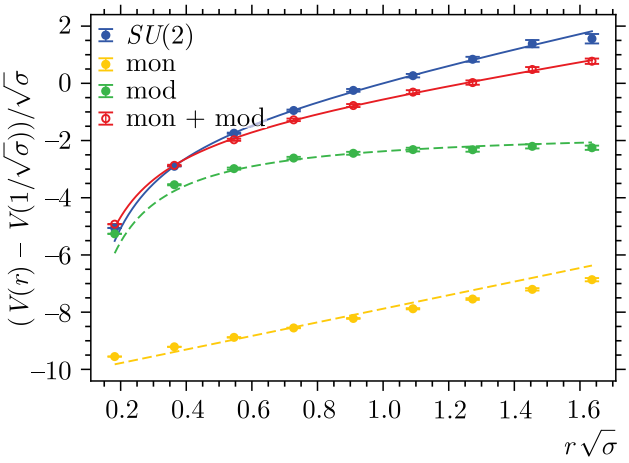


Figure 4. Comparison of the nonabelian potential $V(r)$ (blue) with the monopole potential $V_{\rm mon}(r)$ (yellow), the modified potential $V_{\rm mod}(r)$ (green) and the sum $V_{\rm mod}(r) + V_{\rm mon}(r)$ (red) for the adjoint representation $\beta = 2.5$. The solid curve and dashed curves carry the same meaning as in Figure 2. The plot is shifted as in Figure 2.

and is shown in Figure 3 (left). This plot shows that, indeed, the decomposition improves in the continuum limit.

It is important to demonstrate that such a decomposition is probably not a lattice artifact. For this reason, decomposition was done for another action, theory with dynamical fermions, and potential in the adjoint representation.

The results of the simulation with two flavors of dynamical fermions are shown in the right part of Figure 3, in which case the decomposition is satisfied quite well. It is an open question whether the dynamical quarks are responsible for such an improvement in the accuracy of the decomposition. For the improved action, qualitatively, this decomposition works the same way as that for the potential in the fundamental representation in $SU(2)$ gluodynamics [70]. Figure 4 presents the result for the potential in the adjoint representation, where a similar relation was tested:

$$V_{\rm adj}(r) \approx V_{q2,\rm mon}(r) + V_{\rm adj,mod}(r)\,, \tag{32}$$

where the $SU(2)$ and modified potentials were obtained from Wilson loops in the adjoint representation, and the monopole potentials were obtained from the Wilson loops with charge 2. The decomposition in that case is satisfied with lower precision, which should be checked with better accuracy for several values of β.

5. Decomposition for $SU(3)$ gluodynamics and problem of Gribov copies

In this section, we discuss recent results concerning the decomposition of the gauge field, as well as Abelian and monopole dominance obtained in the MA gauge of $SU(3)$ gluodynamics in [50, 51, 75, 76]. We will demonstrate that, with the proper choice of Gribov copies, one can achieve both Abelian and monopole dominance for the string tension, as well as a decomposition for the static potential.

For gauge group $SU(3)$, the gauge fixing functional for MAG is defined as

$$F(A) = \frac{1}{24V}\int d^4x \sum_{\mu=1}^{4}\sum_{a\neq 3,8} A^a_\mu(x) A^a_\mu(x). \tag{33}$$

The extrema of this functional with respect to gauge transformations $g(x) \in SU(3)/U(1)^2$ satisfy the nonlinear gauge condition

$$D^{ab}_{\mu}(A^i)A^b_{\mu} \equiv \partial_{\mu}A^a_{\mu}(x) - f_{abi}A^i_{\mu}(x)A^b_{\mu}(x) = 0\,, \quad i = 3,8; a,b \neq 3,8\,. \tag{34}$$

The functional (33) has numerous minima, which correspond to Gribov copies.

As in the previous section, we consider the decomposition of the gauge field

$$A_{\mu}(x) = A^{\rm mod}_{\mu}(x) + A^{\rm mon}_{\mu}(x) \tag{35}$$

into the monopole $A^{\rm mon}_{\mu}(x)$ and modified (monopoleless) $A^{\rm mod}_{\mu}(x)$ components after fixing MA gauge and additionally fixing Landau gauge for residual $U(1)\times U(1)$ gauge symmetry. We then check numerically the respective decomposition for the static potential

$$V(r) \approx V^{\rm mod}(r) + V^{\rm mon}(r)\,. \tag{36}$$

In the case of $SU(3)$ gluodynamics, the first result for the decomposition (36) was obtained in [75]. It was shown that the decomposition (36) is satisfied to a good numerical precision. Computations were made for one lattice spacing only, and the fate of this decomposition in the continuum limit of $SU(3)$ gluodynamics was left unchecked. Recently, this gap was closed in [76] as is explained below.

5.1. Details of simulations

The lattice configurations were generated with the Wilson action Eq. (2) for four lattice spacings and a lattice linear size $L \approx 2$ fm. For maximal lattice spacing (at $\beta = 6.0$), two additional lattice sizes were used to study finite volume effects. The parameters of the simulations, including the respective values of the lattice coupling $\beta = 6/g^2$, are presented in Table 3. The lattice spacing values were fixed by values of r_0/a taken from [77].

Table 3. Parameters of the simulations.

β	a, fm	L_s/a	L_s, fm	$N_{\rm conf}$
6.0	0.093	16	1.5	1600
6.0	0.093	24	2.2	5000
6.0	0.093	32	3.0	4000
6.1	0.079	28	2.2	5000
6.1	0.079	36	2.8	14 000
6.2	0.068	32	2.2	3800
6.3	0.059	36	2.1	2100

For the lattice version of MA gauge we use the definition introduced for $SU(3)$ gauge group in [5]. MAG is fixed by minimizing the lattice analogue of the functional (33)

$$F_{\rm lat}(U) = \frac{1}{4\,V}\sum_{x,\mu}\left[1 - \frac{1}{3}(|U^{(11)}_{\mu}(x)|^2 + |U^{(22)}_{\mu}(x)|^2 + |U^{(33)}_{\mu}(x)|^2)\right] = a^2\ F(A) + O(a^4) \tag{37}$$

with respect to local gauge transformations $g(x)$ of the lattice gauge field,

$$U_{\mu}(x) \to U^g_{\mu}(x) = g(x)^{\dagger}U_{\mu}(x)g(x+\hat{\mu})\,. \tag{38}$$

To fix MAG, we used two algorithms described in the previous section: the SA algorithm and the RO algorithm, along with a varying number of random gauge copies $N_{\rm cop}$ to study the effects of Gribov copies. The explanation of the implementation of the SA algorithm in the case of $SU(3)$ gauge group can be found in [28]. Details of another, less effective RO algorithm, can be found in, e.g., [26, 78].

For each gauge field configuration and for each algorithm, we generated $N_{\rm cop}$ independent copies fixed to MA gauge. The copy with a minimal value of the gauge fixing functional will be called the best copy. The gauge noninvariant observables are, in general, dependent on the choice of the Gribov copy. We show the average values of the $F_{\rm lat}$ obtained in our study in Table 4. One can see that these values depend on lattice spacing, volume, and the algorithm. We return to the discussion of the Gribov copy effects later.

Table 4. Values of the functional (37) for $SU(3)$ gluodynamics

L/a	β	$F_{\rm lat}^{\rm RO}$	$F_{\rm lat}^{\rm SA}$
16	6.0	0.267833(25)	0.266046(21)
24	6.0	0.267758(6)	0.265963(5)
32	6.0	0.267745(4)	0.265967(3)
28	6.1	0.257835(5)	0.256363(3)
36	6.1	0.257826(2)	0.256367(1)
32	6.2	0.249020(4)	0.247816(3)
36	6.3	0.241058(5)	0.239930(4)

Next we explain how to make the Abelian projection and define the monopole component of the gauge field for gauge group $SU(3)$ [5]. The Abelian projection means coset decomposition of the nonabelian lattice gauge field $U_\mu(x) \in SU(3)$ into the product

$$U_\mu(x) = U_\mu^{\rm offd}(x) U_\mu^{\rm abel}(x)\,, \tag{39}$$

of the Abelian field $U_\mu^{\rm abel}(x) \in U(1) \times U(1)$ and the coset field $U_\mu^{\rm offd}(x) \in SU(3)/U(1)^2$. The Abelian field $U_\mu^{\rm abel}(x)$ is defined by the maximization of the expression

$$|{\rm Tr}\left(U_\mu^\dagger(x) u_\mu(x)\right)|^2. \tag{40}$$

The solution of this condition is given by [79]

$$U_\mu^{\rm abel}(x) = {\rm diag}\left(u_\mu^{(1)}(x), u_\mu^{(2)}(x), u_\mu^{(3)}(x)\right), \tag{41}$$

where

$$u_\mu^{(a)}(x) = e^{i\theta_\mu^{(a)}(x)} \tag{42}$$

with

$$\theta_\mu^{(a)}(x) = \arg(U_\mu(x))_{aa} - \frac{1}{3}\sum_{b=1}^{3} \arg(U_\mu(x))_{bb}\,\Big|_{\rm mod\ 2\pi} \tag{43}$$

such that

$$\theta_\mu^{(a)}(x) \in [-\frac{4}{3}\pi, \frac{4}{3}\pi] \tag{44}$$

and

$$\sum_a \theta_\mu^{(a)}(x) = 0, \ \mathrm{mod}\ 2\pi. \tag{45}$$

As in case of $SU(2)$ group the Abelian gauge field $U_\mu^{\mathrm{abel}}(x)$ can in turn be decomposed into monopole (singular) and photon (regular) components in the same way as in compact $U(1)$ [71]:

$$\theta_\mu^{(a)}(x) = \theta_\mu^{(a)\,\mathrm{mon}}(x) + \theta_\mu^{(a)\,ph}(x)\,, \tag{46}$$

where

$$\theta_\mu^{(a)\,\mathrm{mon}}(x) = -2\pi \sum_y D(x-y)\partial'_\alpha m_{\alpha\mu}^{(a)}(y)\,. \tag{47}$$

In (47) integer $m_{\mu\nu}^{(a)}(x)$ (Dirac plaquettes) denote the singular part of the Abelian plaquettes

$$\theta_{\mu\nu}^{(a)}(x) \equiv \partial_\mu \theta_\nu^{(a)}(x) - \partial_\nu \theta_\mu^{(a)}(x) = \bar{\theta}_{\mu\nu}^{(a)}(x) + 2\pi m_{\mu\nu}^{(a)}(x)\ ,\ \ \bar{\theta}_{\mu\nu}^{(a)}(x) \in [-\pi, \pi)\,. \tag{48}$$

Then we introduce $U_\mu^{\mathrm{mon}}(x) \in U(1) \times U(1)$:

$$u_\mu^{\mathrm{mon}}(x) = \mathrm{diag}\left(e^{i\theta_\mu^{(1)\,\mathrm{mon}}(x)}, e^{i\theta_\mu^{(2)\,\mathrm{mon}}(x)}, e^{i\theta_\mu^{(3)\,\mathrm{mon}}(x)}\right)\,. \tag{49}$$

Now we can express the decomposition (35) in terms of lattice gauge fields:

$$U_\mu(x) = U_\mu^{\mathrm{mod}}(x)\, u_\mu^{\mathrm{mon}}(x), \tag{50}$$

where $U_\mu^{\mathrm{mod}}(x)$ is the monopoleless component which we also call a modified gauge field. By modification, we understand the removal of the Abelian monopoles.

5.2. The static potential decomposition for the best Gribov copies

We calculated $r \times t$ rectangular Wilson loops $W(r,t)$, $W_{\mathrm{abel}}(r,t)$, $W_{\mathrm{mon}}(r,t)$, and $W_{\mathrm{mod}}(r,t)$ using, respectively, lattice gauge fields $U_\mu(x)$, $U_\mu^{\mathrm{abel}}(x)$, $U_\mu^{\mathrm{mon}}(x)$, and $U_\mu^{\mathrm{mod}}(x)$ introduced above. To reduce the statistical errors in the respective static potentials $V(r)$, $V_{\mathrm{abel}}(r)$, $V_{\mathrm{mon}}(r)$, and $V_{\mathrm{mod}}(r)$, the APE smearing [80] has been employed for spatial links; and in the case of $V(r)$, the hypercubic blocking (HYP) [81] has been employed for temporal links. It is known that at large enough distances r HYP only reduces the divergent selfenergy of $V(r)$. For this reason we used results without blocking for distances $r/a \leqslant 3$ (with the proper constant shift) and results obtained after three HYP sweeps at larger distances.

In Figure 5 (left) we present results for $V_{\mathrm{mon}}(r)$ and $V_{\mathrm{mod}}(r)$ for four lattice spacings (see Table 3) computed using the best copies. These copies were obtained with the SA algorithm and $N_{\mathrm{cop}} = 20$. This implies that we chose Gribov copies which are closest to the global minima of the functional (37). As is known, both for gauge group $SU(2)$ [24, 46, 70] and $SU(3)$ [28, 51] the monopole potential $V_{\mathrm{mon}}(r)$ is linear at large distances and has small curvature at small distances. The modified field potential $V_{\mathrm{mod}}(r)$, as was first demonstrated for $SU(3)$ gluodynamics in [75], is well described by the Coulomb potential. In Figure 5 the potentials were shifted by their values at $r = r_0/2$. Note the weak dependence on the lattice spacing.

In the Figure 5 (right) we compare the gauge invariant static potential $V(r)$ and the sum $V_{\mathrm{mon}}(r) + V_{\mathrm{mod}}(r)$ for the same four lattice spacings. It is clear from the figure that while relation (36) holds to high precision for small distances up to $r/r_0 \leqslant 0.7$, there is no agreement with (36) at large distances. Since we do not see systematic changes with decreasing lattice

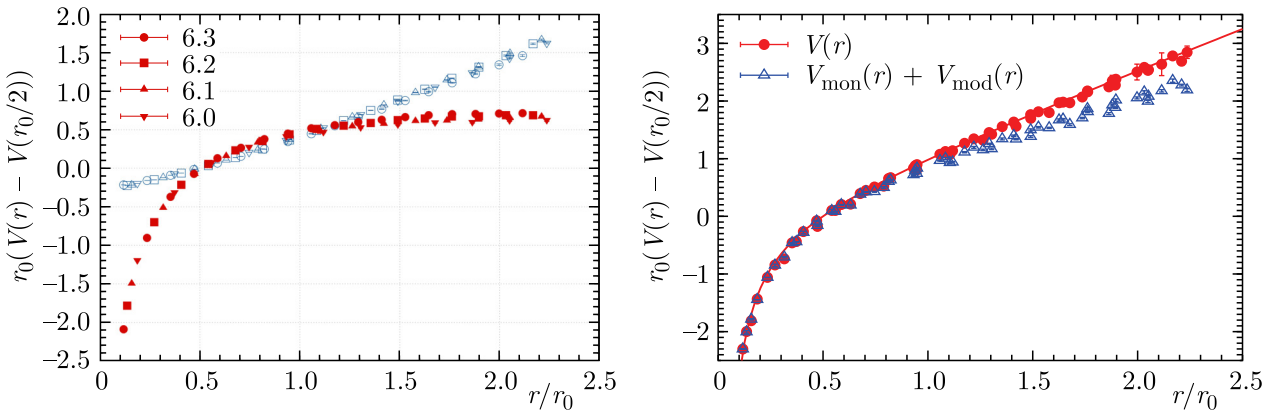


Figure 5. The results for four lattice spacings are shown. Left: $V_{\rm mon}(r)$ (empty symbols) and $V_{\rm mod}(r)$ (filled symbols). Right: comparison between $V(r)$ (filled circles) and $V_{\rm mon}(r)+V_{\rm mod}(r)$ (empty triangles) for the best Gribov copies.

spacing, it is clear that this disagreement does not go away in the continuum limit, contrary to the case of $SU(2)$ gluodynamics [70] described in the previous section.

The large discrepancy between $V(r)$ and the sum $V_{\rm mon}(r)+V_{\rm mod}(r)$ is due to the rather low slope of $V_{\rm mon}(r)$. This low slope is in agreement with the previous results of [28, 49], where Gribov copies close to the global minimum of the gauge fixing functional were also used. In the next section, we will consider another set of Gribov copies to solve this problem.

5.3. Results for selected Gribov copies

In Figure 6 we compare results for $V(r)$ (same as in Figure 5 (right)) with results for $V_{\rm mon}(r) + V_{\rm mod}(r)$ obtained on the same lattices but for a different choice of Gribov copies. This time the Gribov copies were produced using RO algorithm and $N_{\rm cop} = 1$. As one can see from Table 4 the respective functional values are higher in this case. Figure 6 demonstrates that choosing proper Gribov copies it is possible to obtain nice decomposition Eq. (36) for the static potential.

The monopole density is defined as

$$\rho = \frac{\sum_{x,\mu} |k_\mu(x)|}{4V}. \tag{51}$$

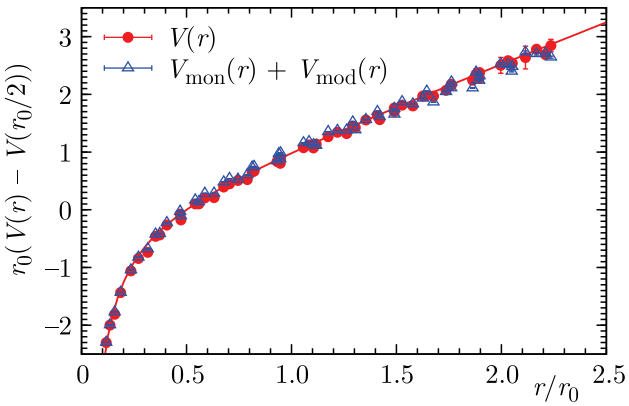


Figure 6. Comparison between $V(r)$ (filled circles) and $V_{\rm mon}(r) + V_{\rm mod}(r)$ (empty triangles) for selected Gribov copies. The data for four lattice spacings is depicted.

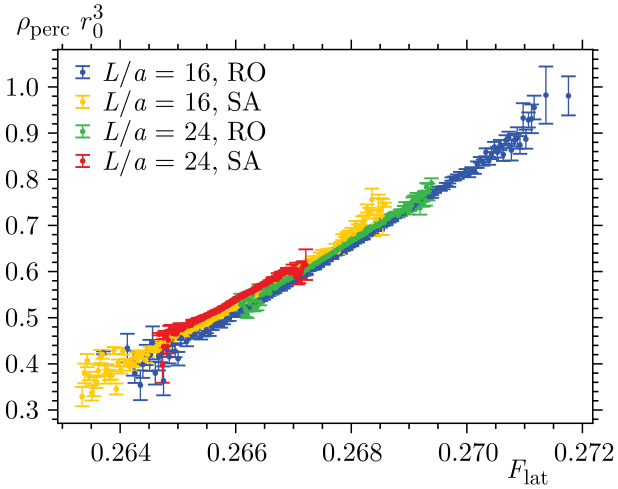


Figure 7. Monopole density for percolating monopole cluster for $\beta = 6.0$ and two lattice sizes: $L/a = 16$ and $L/a = 24$. Both SA results and RO results are shown.

In Figure 7 we show the scatter plot of the density $\rho_{\rm perc}$ for magnetic currents belonging to the percolating cluster vs. the functional $F_{\rm lat}$. The results are presented for two algorithms and for two lattice sizes. These monopoles are also called the infrared monopoles since they determine the infrared properties of the observables like the static potential. One can see that the two algorithms produce very similar values of $\rho_{\rm perc}$ for equal values of $F_{\rm lat}$. But the average value $\langle F_{\rm lat}\rangle$ is different for two algorithms and this difference explains the difference in average values of $\langle\rho_{\rm perc}\rangle$ as well as difference in average values of other observables, including the static potential $V_{\rm mon}(r)$.

The smooth dependence of the monopole density on the functional value seen in Figure 7 is characteristic also for other gauge noninvariant quantities. This indicates that it might be possible to improve further the agreement in Eq. (36), observed in Figure 6, choosing slightly different set of Gribov copies with higher average value of $F_{\rm lat}$.

The importance of Gribov copy effects is also demonstrated in the phenomena of Abelian and monopole dominance. As we explained in Section 3 the equality between σ and σ_{ab} in $SU(3)$ gluodynamics was under question for a long time. The issue was resolved in [50, 51]. In Figure 8, results are shown for the static potential $V(r)$ and for the Abelian static potential $V_{\rm abel}(r)$ computed with the help of the SA algorithm and $N_{\rm cop} = 20$ or with the RO algorithm and $N_{\rm cop} = 1$. It is clear that $V_{\rm abel}(r)$ obtained with the SA algorithm (i.e., for low minima

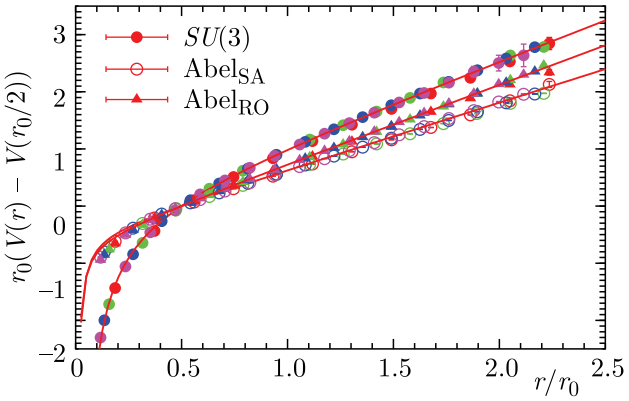


Figure 8. Comparison between $V(r)$ (filled circles) and $V_{\rm abel}(r)$ computed with use of two algorithms: SA (empty circles) and RO (triangles). The data for four lattice spacings is depicted.

of the functional $F_{\rm lat}$) has too small a slope at large distances, while $V_{\rm abel}(r)$ computed on gauge copies obtained with the RO algorithm is parallel to $V(r)$ at large distances. Indeed, the respective ratios are $\sigma_{\rm ab}/\sigma = 0.83(3)$ and $\sigma_{\rm ab}/\sigma = 0.98(3)$. A similar conclusion was made in [50] for the monopole dominance in $SU(3)$ gluodynamics: $\sigma_{\rm mon}/\sigma = 1.01(4)$, i.e., it is close to one for Gribov copies generated via the RO algorithm, while this ratio is only $\sigma_{\rm mon}/\sigma = 0.86(4)$ when the SA algorithm with $N_{\rm cop} = 20$ was used.

To check finite volume effects, we repeated our computations at $\beta = 6.0$ for two more lattices with $L/a = 16$ and 32. We found that the finite volume effects are small. This is in contradiction with results of [45].

5.4. Other decompositions of the gauge field

Next we wish to discuss briefly other decompositions of the gauge field considered in the literature. First, the decomposition into the Abelian and off-diagonal components was suggested in [45]:

$$A_\mu(x) \equiv \sum_{a=1}^{8} A^a_\mu(x) T^a = A^{\rm abel}_\mu(x) + A^{\rm offd}_\mu(x)\,, \tag{52}$$

where $A^{\rm offd}_\mu(x) = \sum_{a\neq 3,8} A^a_\mu(x) T^a$, $A^{\rm abel}_\mu(x) = A^3_\mu(x) T^3 + A^8_\mu(x) T^8$. This decomposition corresponds to the coset decomposition (39) for the lattice gauge field. It was reported in [45] that the sum $V_{\rm abel}(r) + V_{\rm offd}(r)$ approximates well the static potential $V(r)$. This conclusion was checked in [76]. The Gribov copies obtained with RO algorithm were used, and it was found that the sum $V_{\rm abel}(r) + V_{\rm offd}(r)$ reproduced the linear part of the static potential $V(r)$ quite well, but the respective Coulomb part was not reproduced well. Thus, the gauge field decomposition (52) does not lead to good decomposition for the static potential.

One more decomposition of the gauge field appears naturally in the center vortex picture of confinement, see review [13] for definition and results. The lattice gauge field is decomposed into the product of the vortex field $U^{\rm vort}_\mu(x)$ and the modified field $U^{\rm mod,cent}_\mu(x)$:

$$U_\mu(x) = U^{\rm vort}_\mu(x) U^{\rm mod,cent}_\mu(x)\,. \tag{53}$$

The respective static potentials computed from these components of the gauge field are denoted as $V_{\rm vort}(r)$ and $V_{\rm mod,cent}(r)$. The decomposition for the static potential

$$V(r) \approx V_{\rm vort}(r) + V_{\rm mod,cent}(r) \tag{54}$$

was first studied in [72] using the direct central gauge in $SU(2)$ gluodynamics. It was concluded that this decomposition holds with substantially less precision than the decomposition (36), first of all, due to the low string tension provided by the center vortex component. The way to solve the problem with projected string tension $\sigma_{\rm cent}$ in $SU(2)$ gluodynamics, also related to the Gribov copies, was formulated in [14, 82], with promising results. Recently, the static potentials $V_{\rm vort}(r)$ and $V_{\rm mod,cent}(r)$ were studied in $SU(3)$ gluodynamics and in lattice QCD with heavy and light quarks [83]. It was found that in QCD the center-projected string tension $\sigma_{\rm vort}$ is in good agreement with the physical string tension σ but in the gluodynamics $\sigma_{\rm vort}$ is well below σ. Furthermore, the modified component $U^{\rm mod,cent}_\mu(x)$ produces the static potential which is not compatible with the Coulomb potential. These results imply that the decomposition (53) fails to reproduce both the linear term and the Coulomb term of the static potential $V(r)$.

The gauge covariant decomposition of the gauge field was introduced in [84, 85] and further developed in [86–91], see for review [92]. The numerical results demonstrating analogs of the Abelian dominance and the monopole dominance within this approach were obtained in

[93, 94]. It would be interesting to check if the decomposition of the static potential (36) into the monopole and monopoleless components works in this approach.

6. Conclusions

In this paper, we have reviewed recent results on the decomposition of the gauge field into confining (monopole) and non-confining (modified) components in the maximal Abelian gauge, obtained in the context of the dual superconductor scenario of confinement. The decomposition was studied in $SU(2)$ gluodynamics, $SU(2)$ QCD with dynamical fermions, and $SU(3)$ gluodynamics using lattice Monte Carlo simulations.

For $SU(2)$ gluodynamics, the decomposition of the static potential $V(r) \approx V^{\rm mon}(r) + V^{\rm mod}(r)$, corresponding to the gauge field decomposition (26), was demonstrated to hold with good numerical precision for the Wilson action at $\beta = 2.4, 2.5, 2.6$ [70], corresponding to the range of the lattice spacing values $a \in (0.06, 0.12)$ fm. The monopole component $u_\mu^{\rm mon}(x)$ produces the linear part of the potential $V(r)$, while the modified component $\tilde{U}_\mu(x)$ produces the Coulomb part. The relative deviation $\Delta(r)$, defined in Eq. (31), was shown to decrease systematically with increasing β, indicating that the decomposition improves in the continuum limit. The decomposition was also verified for the tadpole improved action and for $SU(2)$ QCD with two flavors of dynamical fermions, where it was satisfied with good accuracy. For the potential in the adjoint representation, the decomposition (32) holds with lower precision, which warrants further investigation at multiple values of β.

For $SU(3)$ gluodynamics, the decomposition (50) was studied at four lattice spacings corresponding to $\beta = 6.0, 6.1, 6.2, 6.3$ [75, 76]. The key finding is that the choice of Gribov copies plays a crucial role. When using Gribov copies closest to the global minimum of the gauge fixing functional (37), obtained with the simulated annealing algorithm, the decomposition does not hold at large distances: the monopole string tension $\sigma^{\rm mon}$ is substantially lower than the physical string tension σ, leading to a significant discrepancy between $V(r)$ and $V^{\rm mon}(r) + V^{\rm mod}(r)$. In contrast, by selecting Gribov copies with a higher average value of the functional — obtained with the relaxation-overrelaxation algorithm — the decomposition is restored to a very good precision. The same choice of Gribov copies also resolves the long-standing question of Abelian and monopole dominance in $SU(3)$ gluodynamics: the ratios $\sigma^{\rm ab}/\sigma = 0.98(3)$ and $\sigma^{\rm mon}/\sigma = 1.01(4)$ were obtained [50, 51], confirming that both Abelian and monopole dominance hold in $SU(3)$ gluodynamics when proper Gribov copies are used. Finite volume effects were checked at $\beta = 6.0$ for three lattice sizes and found to be small, in contradiction with the conclusions of [45].

The analysis of the monopole density ρ, Eq. (51), for the percolating cluster (Figure 7) demonstrated that gauge noninvariant quantities depend continuously on the value of the gauge fixing functional. The two algorithms (SA and RO) produce similar values of $\rho_{\rm perc}$ at equal values of $F_{\rm lat}$, but their different average functional values lead to different average values of $\rho_{\rm perc}$ and other observables, including $V^{\rm mon}(r)$. This continuous dependence suggests that further improvement of the decomposition may be possible by fine-tuning the choice of Gribov copies.

The fact that the MA gauge serves as a tool for locating gauge-invariant Abelian color-magnetic monopoles, as argued in [61], leads to the conclusion that the proper Gribov copies — i.e., those most suitable for observing Abelian and monopole dominance — are different from the global minima of the functional (37), at least in a finite volume. This finding has important implications for the practical implementation of gauge fixing in lattice studies of the dual superconductor scenario.

We also compared the monopole/modified decomposition (50) with other decompositions of the gauge field considered in the literature. The Abelian/off-diagonal decomposition (52) [45], corresponding to the coset decomposition (39), reproduces the linear part of the static potential but fails to reproduce the Coulomb part, as was demonstrated in [76]. The center vortex decomposition (53) in the maximal center gauge suffers from a low string tension of the vortex component and a modified component that is not compatible with a Coulomb potential.

In summary, the lattice results reviewed here provide further support for the dual superconductor scenario of confinement. The monopole component $A_\mu^{\rm mon}(x)$ of the gauge field is responsible for both confinement and chiral symmetry breaking, in the sense that removal of this component destroys the linear part of the static potential and the chiral condensate. The modified (monopoleless) component $A_\mu^{\rm mod}(x)$ is responsible for the Coulomb part of the static potential at all distances, providing a perturbative contribution at small distances and a nonperturbative contribution at large distances.

It is planned to check the decomposition for the static potential in QCD with light quarks. Furthermore, we plan to extend the study of the gauge field decomposition properties on other observables: gauge field and quark propagators, free energy of the static quark-antiquark pair at finite temperature, chiral condensate, hadron masses.

Acknowledgements

This issue of the journal is dedicated to the 70th anniversary of the Joint Institute for Nuclear Research (JINR). Both authors of this review article have personal recollections associated with JINR. One of us (V. B.) began working in lattice QCD after attending a lecture series by V. K. Mitrjushkin at JINR some 40 years ago; he subsequently collaborated successfully with Mitrjushkin and with two other Institute staff members — M. Müller-Preussker and M. Ilgenfritz — who pioneered lattice QCD research at JINR. The scientific career of the second coauthor (I. K.) began under the supervision of V. V. Braguta, who currently heads the lattice QCD group at JINR.

The authors are grateful to T. Suzuki for fruitful discussions. In computations the following computer resources were used: the central Linux-cluster of the A. A. Logunov Institute for High Energy Physics of the Kurchatov Institute (Protvino), the Linux-cluster of KCTEP of the Kurchatov Institute (Moscow), and the Complex of Modeling and Data Processing of Mega-Class Research Facilities of the Kurchatov Institute (Moscow).

Funding

This work was supported by the Russian Science Foundation, grant 23-12-00072-P.

Conflicts of interest

The author declares no conflicts of interest.

References

[1] J. W. Negele, Instantons, the QCD vacuum, and hadronic physics, Nucl. Phys. B Proc. Suppl. 73 (1999) 92–104. arXiv:hep-lat/9810053, doi:10.1016/S0920-5632(99)85010-5.

[2] C. Gattringer, M. Gockeler, P. E. L. Rakow, S. Schaefer, A. Schaefer, A comprehensive picture of topological excitations in finite temperature lattice QCD, Nucl. Phys. B 618 (2001) 205–240. arXiv:hep-lat/0105023, doi:10.1016/S0550-3213(01)00509-0.

[3] V. G. Bornyakov, E. M. Ilgenfritz, B. V. Martemyanov, M. Muller-Preussker, The dyonic picture of topological objects in the deconfined phase, Phys. Rev. D 79 (2009) 034506. arXiv:0809.2142, doi:10.1103/PhysRevD.79.034506.

[4] A. S. Kronfeld, M. L. Laursen, G. Schierholz, U. J. Wiese, Monopole condensation and color confinement, Phys. Lett. B 198 (1987) 516–520. doi:10.1016/0370-2693(87)90910-5.

[5] F. Brandstater, U. J. Wiese, G. Schierholz, Color confinement, Abelian dominance and the dynamics of magnetic monopoles in $SU(3)$ gauge theory, Phys. Lett. B 272 (1991) 319–325. doi:10.1016/0370-2693(91)91837-L.

[6] L. Del Debbio, M. Faber, J. Greensite, S. Olejnik, Center dominance and $Z(2)$ vortices in $SU(2)$ lattice gauge theory, Phys. Rev. D 55 (1997) 2298–2306. arXiv:hep-lat/9610005, doi:10.1103/PhysRevD.55.2298.

[7] P. de Forcrand, M. D'Elia, On the relevance of center vortices to QCD, Phys. Rev. Lett. 82 (1999) 4582–4585. arXiv:hep-lat/9901020, doi:10.1103/PhysRevLett.82.4582.

[8] V. G. Bornyakov, E. M. Ilgenfritz, B. V. Martemyanov, S. M. Morozov, M. Muller-Preussker, A. I. Veselov, Interrelation between monopoles, vortices, topological charge and chiral symmetry breaking: Analysis using overlap fermions for $SU(2)$, Phys. Rev. D 77 (2008) 074507. arXiv:0708.3335, doi:10.1103/PhysRevD.77.074507.

[9] A. Trewartha, W. Kamleh, D. Leinweber, Connection between center vortices and instantons through gauge-field smoothing, Phys. Rev. D 92 (7) (2015) 074507. arXiv:1509.05518, doi:10.1103/PhysRevD.92.074507.

[10] M. N. Chernodub, M. I. Polikarpov, Abelian projections and monopoles, in: NATO Advanced Study Institute on Confinement, Duality and Nonperturbative Aspects of QCD, 1997, pp. 387–414. arXiv:hep-th/9710205.

[11] G. Ripka, Dual superconductor models of color confinement, Lect. Notes Phys. 639 (2004). arXiv:hep-ph/0310102, doi:10.1007/b94800.

[12] M. Chernodub, QCD vacuum as dual superconductor: Quark confinement and topology, Handbook of Nuclear Physics (2023) 1–42. doi:10.1007/978-981-15-8818-1_23-1.

[13] J. Greensite, The confinement problem in lattice gauge theory, Prog. Part. Nucl. Phys. 51 (2003) 1. arXiv:hep-lat/0301023, doi:10.1016/S0146-6410(03)90012-3.

[14] Z. Dehghan, M. Faber, What do we know about the confinement mechanism? Phys. Part. Nucl. 56 (5) (2025) 1148–1154. arXiv:2412.10767, doi:10.1134/S1063779625700236.

[15] H. Suganuma, Quantum chromodynamics, quark confinement, and chiral symmetry breaking: A bridge between elementary particle physics and nuclear physics, Handbook of Nuclear Physics (2023) 1–48. doi:10.1007/978-981-15-8818-1_22-1.

[16] K. G. Wilson, Confinement of quarks, Phys. Rev. D 10 (1974) 2445–2459. doi:10.1103/PhysRevD.10.2445.

[17] J. Kogut, L. Susskind, Hamiltonian formulation of Wilson's lattice gauge theories, Phys. Rev. D 11 (1975) 395–408. doi:10.1103/PhysRevD.11.395.

[18] S. Navas et al., Review of particle physics, Phys. Rev. D 110 (3) (2024) 030001. doi:10.1103/PhysRevD.110.030001.

[19] J. E. Mandula, M. Ogilvie, The gluon is massive: A lattice calculation of the gluon propagator in the Landau gauge, Phys. Lett. B 185 (1987) 127–132. doi:10.1016/0370-2693(87)91541-3.

[20] D. Zwanziger, Quantization of gauge fields, classical gauge invariance and gluon confinement, Nucl. Phys. B 345 (1990) 461–471. doi:10.1016/0550-3213(90)90396-U.

[21] C. Parrinello, G. Jona-Lasinio, A modified Faddeev–Popov formula and the Gribov ambiguity, Phys. Lett. B 251 (1990) 175–180. doi:10.1016/0370-2693(90)90249-6.

[22] D. Zwanziger, Fundamental modular region, Boltzmann factor and area law in lattice theory, Nucl. Phys. B 412 (1994) 657–730. doi:10.1016/0550-3213(94)90396-4.

[23] S. Fachin, C. Parrinello, Global gauge fixing in lattice gauge theories, Phys. Rev. D 44 (1991)

2558–2564. doi:10.1103/PhysRevD.44.2558.

[24] G. S. Bali, V. Bornyakov, M. Muller-Preussker, K. Schilling, Dual superconductor scenario of confinement: A systematic study of Gribov copy effects, Phys. Rev. D 54 (1996) 2863–2875. arXiv:hep-lat/9603012, doi:10.1103/PhysRevD.54.2863.

[25] V. Bornyakov, G. Schierholz, T. Streuer, Glueball and gluelump spectrum in Abelian projected QCD, Nucl. Phys. B Proc. Suppl. 106 (2002) 676–678. arXiv:hep-lat/0111018, doi:10.1016/S0920-5632(01)01813-8.

[26] J. D. Stack, W. W. Tucker, R. J. Wensley, The maximal Abelian gauge, monopoles, and vortices in $SU(3)$ lattice gauge theory, Nucl. Phys. B 639 (2002) 203–222. arXiv:hep-lat/0110196, doi:10.1016/S0550-3213(02)00537-0.

[27] Y. Koma, M. Koma, E.-M. Ilgenfritz, T. Suzuki, A detailed study of the Abelian projected $SU(2)$ flux tube and its dual Ginzburg–Landau analysis, Phys. Rev. D 68 (2003) 114504. arXiv:hep-lat/0308008, doi:10.1103/PhysRevD.68.114504.

[28] V. G. Bornyakov et al. (DIK Collab.), Dynamics of monopoles and flux tubes in two flavor dynamical QCD, Phys. Rev. D 70 (2004) 074511. doi:10.1103/PhysRevD.70.074511.

[29] M. Schröck, H. Vogt, Coulomb, Landau and maximally Abelian gauge fixing in lattice QCD with multi-GPUs, Comput. Phys. Commun. 184 (2013) 1907–1919. doi:10.1016/j.cpc.2013.03.021.

[30] I. L. Bogolubsky, G. Burgio, M. Muller-Preussker, V. K. Mitrjushkin, Landau gauge ghost and gluon propagators in $SU(2)$ lattice gauge theory: Gribov ambiguity revisited, Phys. Rev. D 74 (2006) 034503. arXiv:hep-lat/0511056, doi:10.1103/PhysRevD.74.034503.

[31] V. G. Bornyakov, V. K. Mitrjushkin, M. Muller-Preussker, $SU(2)$ lattice gluon propagator: Continuum limit, finite-volume effects and infrared mass scale m(IR), Phys. Rev. D 81 (2010) 054503. arXiv:0912.4475, doi:10.1103/PhysRevD.81.054503.

[32] G. Burgio, M. Quandt, H. Reinhardt, H. Vogt, Gribov horizon and Gribov copies effect in lattice Coulomb gauge, Phys. Rev. D 95 (1) (2017) 014503. arXiv:1608.05795, doi:10.1103/PhysRevD.95.014503.

[33] L. Del Debbio, M. Faber, J. Giedt, J. Greensite, S. Olejnik, Detection of center vortices in the lattice Yang–Mills vacuum, Phys. Rev. D 58 (1998) 094501. arXiv:hep-lat/9801027, doi:10.1103/PhysRevD.58.094501.

[34] V. G. Bornyakov, D. A. Komarov, M. I. Polikarpov, P-vortices and drama of Gribov copies, Phys. Lett. B 497 (2001) 151–158. doi:10.1016/S0370-2693(00)01309-5.

[35] S. Mandelstam, Vortices and quark confinement in non-Abelian gauge theories, Phys. Rept. 23 (1976) 245–249. doi:10.1016/0370-1573(76)90043-0.

[36] G. 't Hooft, in: 1975 High-Energy Particle Physics Divisional Conference of EPS (includes 8th Biennial Conf. on Elem. Particles), 1975.

[37] G. 't Hooft, Magnetic monopoles in unified gauge theories, Nucl. Phys. B 79 (1974) 276–284. doi:10.1016/0550-3213(74)90486-6.

[38] A. M. Polyakov, Particle spectrum in quantum field theory, JETP Lett. 20 (1974) 194–195.

[39] G. 't Hooft, Topology of the gauge condition and new confinement phases in non-Abelian gauge theories, Nucl. Phys. B 190 (1981) 455–478. doi:10.1016/0550-3213(81)90442-9.

[40] T. A. DeGrand, D. Toussaint, Topological excitations and Monte Carlo simulation of Abelian gauge theory, Phys. Rev. D 22 (1980) 2478–2489. doi:10.1103/PhysRevD.22.2478.

[41] Z. F. Ezawa, A. Iwazaki, Abelian dominance and quark confinement in Yang–Mills theories, Phys. Rev. D 25 (1982) 2681. doi:10.1103/PhysRevD.25.2681.

[42] T. Suzuki, A Ginzburg–Landau type theory of quark confinement, Prog. Theor. Phys. 80 (1988) 929. doi:10.1143/PTP.80.929.

[43] S. Hioki, S. Kitahara, S. Kiura, Y. Matsubara, O. Miyamura, S. Ohno, T. Suzuki, Abelian dominance in $SU(2)$ color confinement, Phys. Lett. B 272 (1991) 326–332. doi:10.1016/0370-2693(91)91838-M.

[44] V. Bornyakov, M. Muller-Preussker, Continuum limit in Abelian projected $SU(2)$ lattice gauge theory, Nucl. Phys. B Proc. Suppl. 106 (2002) 646–648. arXiv:hep-lat/0110209, doi:10.1016/S0920-5632(01)01803-5.

[45] N. Sakumichi, H. Suganuma, Perfect Abelian dominance of quark confinement in $SU(3)$ QCD, Phys. Rev. D 90 (11) (2014) 111501. doi:10.1103/PhysRevD.90.111501.

[46] H. Shiba, T. Suzuki, Monopoles and string tension in $SU(2)$ QCD, Phys. Lett. B 333 (1994) 461–466. arXiv:hep-lat/9404015, doi:10.1016/0370-2693(94)90168-6.

[47] J. D. Stack, S. D. Neiman, R. J. Wensley, String tension from monopoles in $SU(2)$ lattice gauge theory, Phys. Rev. D 50 (1994) 3399–3405. arXiv:hep-lat/9404014, doi:10.1103/PhysRevD.50.3399.

[48] R. W. Haymaker, Confinement studies in lattice QCD, Phys. Rept. 315 (1999) 153–173. arXiv:hep-lat/9809094, doi:10.1016/S0370-1573(99)00019-8.

[49] V. G. Bornyakov, M. I. Polikarpov, M. N. Chernodub, T. Suzuki, G. Schierholz, Color confinement and hadron structure in lattice chromodynamics, Phys. Usp. 47 (2004) 17–35. doi:10.1070/PU2004v047n01ABEH001605.

[50] I. E. Kudrov, V. G. Bornyakov, Gribov copy effects in the maximal Abelian gauge, Phys. Part. Nucl. 56 (2) (2025) 242–246. arXiv:2409.00691, doi:10.1134/S1063779624701478.

[51] I. Kudrov, V. Bornyakov, Abelian and monopole dominance in $SU(3)$ gluodynamics and Gribov copy effects, Phys. Part. Nucl. Lett. 22 (1) (2025) 112–116. arXiv:2503.15075, doi:10.1134/S1547477124701930.

[52] F. X. Lee, R. M. Woloshyn, H. D. Trottier, Abelian dominance of chiral symmetry breaking in lattice QCD, Phys. Rev. D 53 (1996) 1532–1536. arXiv:hep-lat/9509028, doi:10.1103/PhysRevD.53.1532.

[53] H. Ohata, H. Suganuma, Clear correlation between monopoles and the chiral condensate in $SU(3)$ QCD, Phys. Rev. D 103 (5) (2021) 054505. arXiv:2012.03537, doi:10.1103/PhysRevD.103.054505.

[54] H. Suganuma, H. Ohata, Local correlation among the chiral condensate, monopoles, and color magnetic fields in Abelian projected QCD, Universe 7 (9) (2021) 318. arXiv:2108.08499, doi:10.3390/universe7090318.

[55] S. Sasaki, O. Miyamura, A conclusive test of Abelian dominance hypothesis for topological charge in the QCD vacuum, Nucl. Phys. B Proc. Suppl. 73 (1999) 545–547. arXiv:hep-lat/9808019, doi:10.1016/S0920-5632(99)85132-9.

[56] V. G. Bornyakov, A. G. Kononenko, V. K. Mitrjushkin, Study of thermal monopoles in lattice QCD, PoS LATTICE2013 187 (2014) 358. arXiv:1312.4085, doi:10.22323/1.187.0358.

[57] A. D'Alessandro, M. D'Elia, E. V. Shuryak, Thermal monopole condensation and confinement in finite temperature Yang–Mills theories, Phys. Rev. D 81 (2010) 094501. arXiv:1002.4161, doi:10.1103/PhysRevD.81.094501.

[58] F. V. Gubarev, E.-M. Ilgenfritz, M. I. Polikarpov, T. Suzuki, The lattice $SU(2)$ confining string as an Abrikosov vortex, Phys. Lett. B 468 (1999) 134–137. arXiv:hep-lat/9909099, doi:10.1016/S0370-2693(99)01208-3.

[59] Y. Koma, M. Koma, E.-M. Ilgenfritz, T. Suzuki, M. I. Polikarpov, Duality of gauge field singularities and the structure of the flux tube in Abelian projected $SU(2)$ gauge theory and the dual Abelian Higgs model, Phys. Rev. D 68 (2003) 094018. arXiv:hep-lat/0302006, doi:10.1103/PhysRevD.68.094018.

[60] P. Cea, L. Cosmai, F. Cuteri, A. Papa, Flux tubes in the $SU(3)$ vacuum: London penetration depth and coherence length, Phys. Rev. D 89 (9) (2014) 094505. arXiv:1404.1172, doi:10.1103/PhysRevD.89.094505.

[61] C. Bonati, A. Di Giacomo, M. D'Elia, Detecting monopoles on the lattice, Phys. Rev. D 82 (2010) 094509. doi:10.1103/PhysRevD.82.094509.

[62] A. Di Giacomo, G. Paffuti, A disorder parameter for dual superconductivity in gauge theories, Phys. Rev. D 56 (1997) 6816–6823. arXiv:hep-lat/9707003, doi:10.1103/PhysRevD.56.6816.

[63] A. Di Giacomo, B. Lucini, L. Montesi, G. Paffuti, Color confinement and dual superconductivity of the vacuum, Phys. Rev. D 61 (2000) 034503. arXiv:hep-lat/9906024, doi:10.1103/PhysRevD.61.034503.

[64] C. Bonati, G. Cossu, M. D'Elia, A. Di Giacomo, The disorder parameter of dual superconductivity in QCD revisited, Phys. Rev. D 85 (2012) 065001. arXiv:1111.1541, doi:10.1103/PhysRevD.85.065001.

[65] A. Di Giacomo, A gauge invariant order parameter for monopole condensation in QCD vacuum, JHEP 02 (2021) 208. arXiv:2010.04232, doi:10.1007/JHEP02(2021)208.

[66] J. Frohlich, P. A. Marchetti, Soliton quantization in lattice field theories, Commun. Math. Phys. 112 (1987) 343–383. doi:10.1007/BF01217817.

[67] T. Suzuki, K. Ishiguro, Y. Koma, T. Sekido, Gauge-independent Abelian mechanism of color confinement in gluodynamics, Phys. Rev. D 77 (2008) 034502. arXiv:0706.4366, doi:10.1103/PhysRevD.77.034502.

[68] A. Hiraguchi, K. Ishiguro, T. Suzuki, New Abelian-like monopoles and the dual Meissner effect, Phys. Rev. D 102 (2020) 114504. arXiv:2011.14377, doi:10.1103/PhysRevD.102.114504.

[69] K. Ishiguro, A. Hiraguchi, T. Suzuki, Monopoles of the Dirac type and color confinement in QCD: First results of $SU(3)$ numerical simulations without gauge fixing, Phys. Rev. D 106 (1) (2022) 014515. arXiv:2207.04436, doi:10.1103/PhysRevD.106.014515.

[70] V. G. Bornyakov, I. Kudrov, R. N. Rogalyov, Decomposition of the $SU(2)$ gauge field in the maximal Abelian gauge, Phys. Rev. D 105 (5) (2022) 054519. doi:10.1103/PhysRevD.105.054519.

[71] J. Smit, A. van der Sijs, Monopoles and confinement, Nucl. Phys. B 355 (1991) 603–648. doi:10.1016/0550-3213(91)90489-K.

[72] V. G. Bornyakov, M. I. Polikarpov, G. Schierholz, T. Suzuki, S. N. Syritsyn, New features of the maximal Abelian projection, Nucl. Phys. B Proc. Suppl. 153 (2006) 25–32. arXiv:hep-lat/0512003, doi:10.1016/j.nuclphysbps.2006.01.002.

[73] V. G. Bornyakov, V. V. Braguta, E. M. Ilgenfritz, A. Y. Kotov, A. V. Molochkov, A. A. Nikolaev, Observation of deconfinement in a cold dense quark medium, JHEP 03 (2018) 161. arXiv:1711.01869, doi:10.1007/JHEP03(2018)161.

[74] G. S. Bali, V. Bornyakov, M. Muller-Preussker, F. Pahl, New algorithm for gauge fixing in $SU(2)$ lattice gauge theory, Nucl. Phys. B Proc. Suppl. 42 (1995) 852–854. arXiv:hep-lat/9412027, doi:10.1016/0920-5632(95)00401-T.

[75] V. G. Bornyakov, I. E. Kudrov, Decomposition of the static potential in $SU(3)$ gluodynamics, JETP Lett. 117 (5) (2023) 328–331. arXiv:2301.03076, doi:10.1134/S0021364023600209.

[76] V. Bornyakov, V. Goy, I. Kudrov, New results on gauge field decomposition in $SU(3)$ gluodynamics (6 2026). arXiv:2606.13490.

[77] S. Necco, R. Sommer, The $N_f = 0$ heavy quark potential from short to intermediate distances, Nucl. Phys. B 622 (2002) 328–346. doi:10.1016/S0550-3213(01)00582-X.

[78] M. Schröck, H. Vogt, Gauge fixing in lattice QCD with multi-GPUs, Acta Phys. Polon. Supp. 6 (3) (2013) 763–768. arXiv:1305.3440, doi:10.5506/APhysPolBSupp.6.763.

[79] V. G. Bornyakov et al., Finite temperature QCD with two flavors of nonperturbatively improved Wilson fermions, Phys. Rev. D 71 (2005) 114504. arXiv:hep-lat/0401014, doi:10.1103/PhysRevD.71.114504.

[80] M. Albanese et al., Glueball masses and string tension in lattice QCD, Phys. Lett. B 192 (1987) 163–169. doi:10.1016/0370-2693(87)91160-9.

[81] A. Hasenfratz, F. Knechtli, Flavor symmetry and the static potential with hypercubic blocking, Phys. Rev. D 64 (2001) 034504. doi:10.1103/PhysRevD.64.034504.

[82] Z. Dehghan, R. Golubich, R. Höllwieser, M. Faber, Investigation of the ensemble of maximal center gauge, Phys. Rev. D 110 (1) (2024) 014501. arXiv:2404.13304, doi:10.1103/PhysRevD.110.014501.

[83] J. C. Biddle, W. Kamleh, D. B. Leinweber, Static quark potential from center vortices in the presence of dynamical fermions, Phys. Rev. D 106 (5) (2022) 054505. arXiv:2206.00844, doi:10.1103/PhysRevD.106.054505.

[84] Y. M. Cho, A restricted gauge theory, Phys. Rev. D 21 (1980) 1080. doi:10.1103/PhysRevD.21.1080.

[85] Y.-S. Duan, M.-L. Ge, $SU(2)$ gauge theory and electrodynamics with N magnetic monopoles, Sci. Sin. 9 (11) (1979). doi:10.1142/9789813237278_0001.

[86] L. D. Faddeev, A. J. Niemi, Partially dual variables in $SU(2)$ Yang–Mills theory, Phys. Rev. Lett. 82 (1999) 1624–1627. arXiv:hep-th/9807069, doi:10.1103/PhysRevLett.82.1624.

[87] S. V. Shabanov, An effective action for monopoles and knot solitons in Yang–Mills theory, Phys. Lett. B 458 (1999) 322–330. arXiv:hep-th/9903223, doi:10.1016/S0370-2693(99)00612-7.

[88] S. V. Shabanov, Yang–Mills theory as an Abelian theory without gauge fixing, Phys. Lett. B 463 (1999) 263–272. arXiv:hep-th/9907182, doi:10.1016/S0370-2693(99)01024-2.

[89] K. I. Kondo, T. Murakami, T. Shinohara, Yang–Mills theory constructed from Cho–Faddeev–Niemi decomposition, Prog. Theor. Phys. 115 (2006) 201–216. arXiv:hep-th/0504107, doi:10.1143/PTP.115.201.

[90] S. Kato, K. I. Kondo, T. Murakami, A. Shibata, T. Shinohara, S. Ito, Lattice construction of Cho–Faddeev–Niemi decomposition and gauge invariant monopole, Phys. Lett. B 632 (2006) 326–332. arXiv:hep-lat/0509069, doi:10.1016/j.physletb.2005.10.089.

[91] N. Cundy, Y. M. Cho, W. Lee, J. Leem, The static quark potential from the gauge invariant Abelian decomposition, Phys. Lett. B 729 (2014) 192–198. arXiv:1307.3085, doi:10.1016/j.physletb.2014.01.009.

[92] K.-I. Kondo, S. Kato, A. Shibata, T. Shinohara, Quark confinement: Dual superconductor picture based on a non-Abelian Stokes theorem and reformulations of Yang–Mills theory, Phys. Rept. 579 (2015) 1–226. arXiv:1409.1599, doi:10.1016/j.physrep.2015.03.002.

[93] S. Kato, K.-I. Kondo, A. Shibata, Gauge-independent "Abelian" and magnetic-monopole dominance, and the dual Meissner effect in lattice $SU(2)$ Yang–Mills theory, Phys. Rev. D 91 (3) (2015) 034506. arXiv:1407.2808, doi:10.1103/PhysRevD.91.034506.

[94] N. Cundy, Y. M. Cho, W. Lee, J. Leem, The static quark potential from the gauge independent Abelian decomposition, Nucl. Phys. B 895 (2015) 64–131. arXiv:1503.07033, doi:10.1016/j.nuclphysb.2015.03.027.